Polymer 51 (2010) 3262–3268

Contents lists available at ScienceDirect

Polymer

journal homepage: www.elsevier.com/locate/polymer

Linear viscoelasticity of polymer melts filled with nano-sized fillers

Yihu Song*, Qiang Zheng

Key Laboratory of Macromolecular Synthesis and Functionalization of Ministry of Education, Department of Polymer Science and Engineering, Zhejiang University, Hangzhou 310027, China

ARTICLE INFO

Article history:
Received 7 November 2009
Received in revised form
28 April 2010
Accepted 9 May 2010
Available online 15 May 2010

Keywords:
Polymers
Nanofillers
Linear viscoelasticity

ABSTRACT

The linear dynamic rheology of polymer melts filled with nano-sized fillers is investigated in relation to a proposed two phase model. A common principle is disclosed for nanofilled polymers exhibiting either fluid- or solid-like behaviors with increasing filler volume fraction. The bulky polymer phase far away from the filler inclusions in the nanocomposites behaves the same as in the unfilled case while its contribution to the composite modulus is enlarged due to strain amplification effect. The filler forms aggregates together with polymer chains absorbed on the filler surface, which is termed as the "filler phase" in the proposed model. The dynamics of the "filler phase" slow down with increasing filler concentration. The applicability of the proposed two phase model is discussed in relation to the well-known structural inhomogeneity of nanofilled polymers as well as the strain amplification and the filler clustering effects.

1. Introduction

Filled polymers exhibit a diverse range of rheological properties, varying from simple viscous fluids to highly elastic solids with increasing filler volume fraction, φ. The effect of filling on rheology is well-known in the range of small φ where the reinforcement could be attributed to hydrodynamic effects caused by the solid inclusions in the melt stream [1–3]. For high φ where direct particle contacts dominate the deformation, a straightforward solution of hydrodynamic equations is difficult and theoretical models based on realistic structural ideas are missing so far.

Filled polymers usually show strong flow as well as strain and temperature history dependent rheological behaviors. It is always important to determine the dynamic viscoelastic properties at a strain that is low enough not to affect the material response [4]. Small strain-amplitude frequency sweep is usually used to collect linear rheological data which are reproductive for repeated measurements within a certain experimental error [5]. Linear rheology is a way generally used to assess the state of dispersion of fillers in the melt [6]. Large increases in complex modulus $G^*(\omega)$ and complex viscosity $\eta^*(\omega)$ as well as appearance of a terminal modulus plateau in the low-frequency (ω) zone have been commonly observed in filled polymers. In nanocomposites, the terminal plateau can even be observed at considerably low φ. Though the exact mechanism is not clear, the solid-like behavior is generally assigned to originations differing from the liquid-like rheology at low φ. The liquid- to solid-like transition at the low-ω zone has been ascribed to the slowdown of chain relaxation due to polymer adsorption on the surface of particles [7–10], the long-lived chain bridges between the particles [11,12], the jammed network [13] of interacting particles at low and intermediate φ [14,15], or the colloidal and frictional interactions [15] as well as breakdown of lubricated indirect contacts between particles at φ high enough [16]. In highly filled polymers, solid-like yielding can be observed even at temperatures above the quiescent melting temperature (T_m) or glass transition temperature (T_g) of the polymer [17].

Dynamic rheology in the linearity regime is sensitive to filler dispersion in polymers [18]. However, a straightforward description of how linear rheology varies with φ is still missing so far. In this article, we systematically study the linear rheology of different nanofilled polymers by analyzing storage modulus $G'(\omega)$ and loss modulus $G''(\omega)$. The nanocomposites under consideration include carbon black (CB) filled high-density polyethylene (HDPE) and ethylene-tetrafluoroethylene (ETFE) alternating copolymer investigated in our laboratory [19], fumed silica filled polystyrene (PS) by Havet and Isayev [20], precipitated silica filled polydimethylsiloxane (PDMS) by Shim and Isayev [21], silicon dioxide (SiO_2) nanoparticle filled PS by Filippone et al. [22], carbon nanofiber (CNF) filled PS by Wang et al. [23], multi-walled carbon nanotube (MWCNT) filled poly (butylene terephthalate) (PBT) by Wu et al. [24], and clay filled linear low-density polyethylene (LLDPE) by Durmus et al. [25]. The data were taken from published reports in which linear rheology of the matrix was located in the terminal region and the data were

* Corresponding author. Fax: +86 571 8793075.
E-mail address: s_yh0411@zju.edu.cn (Y. Song).

0032-3861/$ – see front matter © 2010 Elsevier Ltd. All rights reserved.
doi:10.1016/j.polymer.2010.05.018

represented in double logarithmic plot so that the data points of any composition could be clearly read.

The paper is organized as follows. In Section 2 we propose a two phase model to account for the linear rheology of nanofilled polymers. In Section 3 we describe how the proposed model works in the different nanocomposites under consideration. In Section 4 we discuss the structural difference of the filler phase to account for the underlying physical mechanisms of the linear rheology of nanofilled polymers on the basis of the proposed model.

2. The two phase model

The presence of hard and much less deformable filler inclusions in a soft and highly deformable matrix leads to hydrodynamic effects referring to a strain amplification factor A_f [26]. A_f can be experimentally determined [27–30] and is used to account for the reinforcement of filled elastomers [31] and the dynamic moduli in the high-ω zone [7]. The global straining on the filled polymer is concentrated in the interstitial fluid [1] so that the local strain of the interstitial fluid must exceed the macroscopic strain. Continuum mechanical theories assuming a perfectly bonded interface between the matrix and the rigid inclusions predict an effective complex modulus [32].

$$G^*(\omega,\varphi) = A_f(\omega,\varphi)G^*_m(\omega) \tag{1}$$

Here, $G^*_m(\omega)$ is complex modulus of the unfilled polymer. The variable $A_f(\omega,\varphi)$ depending on both ω and φ represents the modulus enhancement arising from the inhomogeneous strain field created by the rigid inclusions. It should be the norm that A_f is independent of ω considering the structural relaxation of the filler phase does not occur at normally achieved test frequencies. The contribution of the matrix to the composite modulus is thus expressed as $A_f(\varphi)G^*_m(\omega)$ in the whole ω domain.

Except for the hydrodynamic reinforcement, filler inclusions at φ high enough are connected to each other by direct contacts as well as by bridging of polymer chains adsorbed on separate aggregates, leading to the formation of filler clusters on a large scale and even a filler network superimposed on the molecular network [33]. The modulus plateau at the terminal flow zone is indicative of the filler structure [34]. Elastically stretched nanoparticle chainlike aggregates (NCA) provide a direct support for the filler networking [35–38]. NCA undergoes plastic deformation and breakage midway along its length at large strains [37] while it behaves elastically at small strains [39]. In particular, CB exists as folded chains in polymer while the CB chains are unfolded upon stretching. Chains in a NCA network behave elastically similar to an individual NCA [37]. In filled polymers, the overlapping aggregates are interconnected by particle chains continuously created and broken down due to thermal processes [5]. The backbone of filler aggregates is able to respond to small deformations as a contorted rigid rod, and is responsible for the elastic behavior at rest, which has been modeled as an interconnected bundle of chains of particles [40]. The filler phase contributes a complex modulus $G^*_f(\omega,\varphi) = G'_f(\omega,\varphi) + iG''_f(\omega,\varphi)$ related to the elastically rigid interaggregate chains. A microrheological model based on the fractal concept reveals that $G'_f(\omega,\varphi)$ is very weakly dependent on ω while $G''_f(\omega,\varphi)$ is approximately independent of ω [5], say

$$G^*_f(\omega,\varphi) = G'_{f1}(\varphi)\omega^\alpha + iG''_{f0}(\varphi) \tag{2}$$

Here, α is an exponent, $G'_{f1}(\varphi)$ is storage modulus of the filler phase at $\omega = 1$ rad s^{-1} and $G''_{f0}(\varphi)$ is a constant representing the viscous contribution of the filler phase.

The shear stress in the suspensions can be divided into certain hydrodynamic and structural contributions of aggregates [5,40]. Both the filler and the polymer contribute independently to modulus; the total rheological response is the sum of the two independent contributions, with the contributions of the filler and the polymer phases varying significantly with φ. The effective complex modulus of filled polymers is related to those of the pure polymer and the filler phase.

$$G^*(\omega,\varphi) = A_f(\varphi)G^*_m(\omega) + G^*_f(\omega,\varphi) \tag{3}$$

Influence of filler to the molecular dynamics is an intriguing and contradictory question. It largely depends on the polymer–filler affinity. Filling might induce increase, decrease, or no change in T_g [41–43] depending on the polymer–filler interactions [39,44]. Some filled polymers may exhibit two populations of relaxation time [45] or two T_g transitions [46–49] associated with the normal segmental dynamics of the bulk polymer and the restricted mobility of chains adjacent to the filler surface, respectively. A layer of loosely bound chains, in addition to the immobile layer and the unrestricted bulk polymer, has also been detected in some systems [50]. Molecular dynamics simulation also suggests a many-layer model associated with a gradual change of the polymer dynamics approaching the nanoparticle surface [51]. However, other studies reveal that reinforcing particles generally have a negligible effect on the interfacial segmental dynamics [43]. In nano-sized silica filled poly(vinyl acetate), local segmental dynamics of the chains adjacent to particles do not differ from the bulk chains even though amounts of bound and occluded polymers increase with φ [52]. Small angle neutron scattering studies on PS loaded with spherical silica nanoparticles unequivocally disclose unperturbed chain conformations independent of φ [53].

Unusually strong and pervasive interfacial interactions unambiguously results in a “rubber shell” that exhibits restricted chain mobility in comparison with the bulk [17,43,54–56]. Computer simulations reveal that nanoparticles can influence the viscoelasticity of polymer melt by modifying the relaxation spectrum, slowing down relaxations of the polymers and distorting the strain field around the particles [8,32,57]. The polymer–polymer, particle–particle and polymer–particle interactions have been included into phenomenological [23,41,58–61] and molecular models [62,63] proposed for accounting for the linear rheology of filled polymers. Microscopic models based on glassy layers around the fillers are proposed for interpreting the high level of stress between fillers [55,56,64].

However, the proposed immobilized polymer layer concept does not appear to have much relevance to the overall viscoelasticity of filled polymers [65]. It is generally accepted that, in filled polymers, the dynamics of polymer segments strictly restricted in the vicinity of the particles might be inhomogeneously retarded while polymer segments far away from the particles exhibit the bulk behavior. The chain immobilization, by either physical or chemical absorption, or by chain confinement in nanoclay composites, and the boundary interphase, if it exists, are localized in the close vicinity of the filler surface.

The interphase plays a decisive role in determination of the viscoelasticity of filled polymers. Three phase model has been introduced in self-consistent models for accounting for the “particle-interphase-matrix” morphology of filled polymers. From a theoretical point of view, it is reasonable to adopt the two phase model incorporating the interphase layer into the filler phase by neglecting the rigidity difference of the particle and the interphase layer [66]. In the proposed two phase model, the immobilized chains and the possible interphase might be included in the filler phase nominally. Any variations in polymer dynamics localized in

the close vicinity of the filler particles do not affect the viscoelasticity of the bulky polymer phase away from the particles. The dimension of an interphase varies greatly from system to system, depending on the polymer–filler affinity [67] and filler concentration [68]. By including interphase into the "filler phase", the approach can be applied to non-interacting and highly interacting polymer–filler systems. This concept could be referred to the micromechanical approaches using 'coated' particles (hard particle core plus bound polymer layer) [69] or Eshelby's equivalent inclusion (randomly dispersed spherical fillers covered by interphase layer) [70] for prediction of effective elastic moduli of filled polymers.

3. Application of the model

Fig. 1 shows master curves of linear rheology at 160 °C for CB/HDPE nanocomposites prepared via melt blending (MB) method [19]. In the high-ω zone above 1 rad s^{-1}, the modulus curves of the nanocomposites are nearly parallel to the respective curves of the pure polymer. In the low-ω zone below 10^{-2} rad s^{-1}, HDPE exhibits the typical terminal flow characterized by $G'_m(\omega) \sim \omega^2$ and $G''_m(\omega) \sim \omega^1$. Addition of CB elevates moduli over the whole ω range. The viscoelastic response is mainly altered in the low-ω zone, where $G'(\omega, \varphi)$ and $G''(\omega, \varphi)$ exhibit diminished ω-dependences in comparison with the neat polymer behavior. Modulus plateaus are observed at $\varphi = 0.13$ and the nanocomposite is characterized by $G' \approx G''$ in the terminal region. The $G'(\omega, \varphi)$ and $G''(\omega, \varphi)$ curves form two crossovers at $\varphi = 0.13$ while only one crossover is observed at $\varphi < 0.13$.

Polynomial functions

$$G'_m(\omega) = \sum_j g'_j \omega^j \tag{4a}$$

and

$$G''_m(\omega) = \sum_j g''_j \omega^j \tag{4b}$$

were used to fit $G'_m(\omega)$ and $G''_m(\omega)$ of the matrix polymer using least square fitting method. Here g'_j and g''_j are coefficients

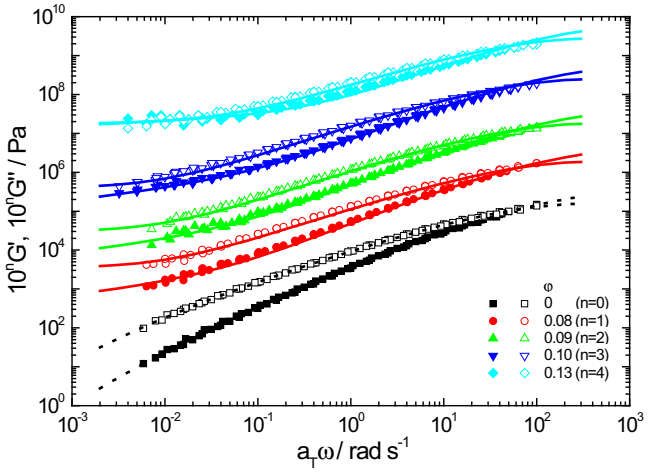

Fig. 1. Master curves of G' (solid symbols) and G'' (hollow symbols) as a function of scaled frequency $a_T\omega$ for CB/HDPE nanocomposites at 160 °C. The data of G' and G'' are vertically shifted by a factor of 10^n. The data measured at 180 °C, 200 °C and 220 °C were shifted horizontally by a shift factor a_T to superpose the data at 160 °C. The data were taken from our previous work [19]. The dotted curves are drawn according to least square fitting of Eq. (4) with $j = 3$ to the pure polymer and solid curves are calculated according to Eq. (5).

associated with the j-th power. The fitting is a phenomenological treatment and a coefficient of determination above 0.9999 could be obtained with $j \geq 3$. For simplifying the fitting procedure, the polynomial functions up to $j = 3$ was applied. Eq. (3) was then modified as

$$G'(\omega, \varphi) = A_f(\varphi) \sum_{j=0}^{3} g'_j \omega^j + G'_{fl}(\varphi)\omega^\alpha \tag{5a}$$

$$G''(\omega, \varphi) = A_f(\varphi) \sum_{j=0}^{3} g''_j \omega^j + G''_{f0}(\varphi) \tag{5b}$$

Eq. (5b) with two unknown adjusting parameters, $A_f(\varphi)$ and $G''_{f0}(\varphi)$, was applied to fit $G''(\omega, \varphi)$ and then, Eq. (5a) with α and $G'_{f1}(\varphi)$ as adjusting parameters is applied to fit $G'(\omega, \varphi)$ of the nanocomposites. By such procedure, we can determine all the four parameters, $A_f(\varphi)$, α, $G'_{f1}(\varphi)$ and $G''_{f0}(\varphi)$. The best fitted results shown as solid curves in Fig. 1 well describe the viscoelasticity of the nanocomposites in the ω range achieved.

Fig. 2 shows the linear rheology of SiO_2/PS nanocomposites prepared by the MB method [22]. The general rheological characteristics are similar to Fig. 1. In the terminal region, $G'(\omega, \varphi)$ exceeds $G''(\omega, \varphi)$ at $\varphi \geq 0.028$. Modulus plateau is observed at $\varphi = 0.04$ and $\varphi = 0.05$. The $G'(\omega, \varphi)$ and $G''(\omega, \varphi)$ curves form one crossover at low concentrations and two crossovers at $\varphi = 0.028$ and 0.040. On the other hand, there is no G'–G'' crossover ($G' > G''$ in the whole ω domain) at $\varphi = 0.050$. Despite the differences between the SiO_2/PS and the HDPE/CB nanocomposites, the linear rheology in Fig. 2 could also be well described by Eq. (3).

Wang et al. [23] prepared CNF/PS nanocomposites using the MB and the solvent casting (SC) methods. The linear rheology of the nanocomposites is shown in Fig. 3. The mechanical damage during melt blending causes CNF to become shorter (1–20 μm) than CNF in the SC nanocomposites (4–60 μm). The modulus increment with φ is more significant in the SC nanocomposites than in the MB nanocomposites. In the MB nanocomposites, the G'–G'' crossover frequency, ω_{cr}, shifts very slightly towards low frequencies with increasing φ to 0.058 (10 wt%). On the other hand, in the SC nanocomposites, ω_{cr} shifts more than one decade at $\varphi = 0.058$. Wang et al. argued that the characteristic relaxation time increases with φ and, for the SC nanocomposites at $\varphi = 0.058$, it becomes nine

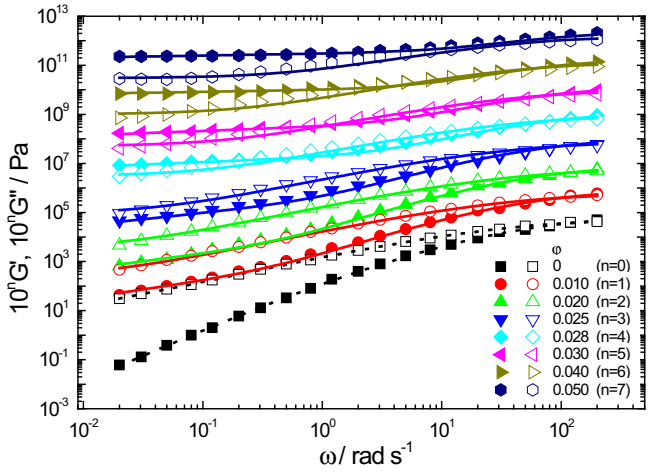

Fig. 2. G' (solid symbols) and G'' (hollow symbols) as a function of frequency ω for SiO_2/PS nanocomposites. The data of G' and G'' are vertically shifted by a factor of 10^n. G' and G'' were taken from Filippone et al. [22]. The dotted curves are drawn according to least square fitting of Eq. (4) with $j = 3$ to the pure polymer and solid curves are calculated according to Eq. (5).

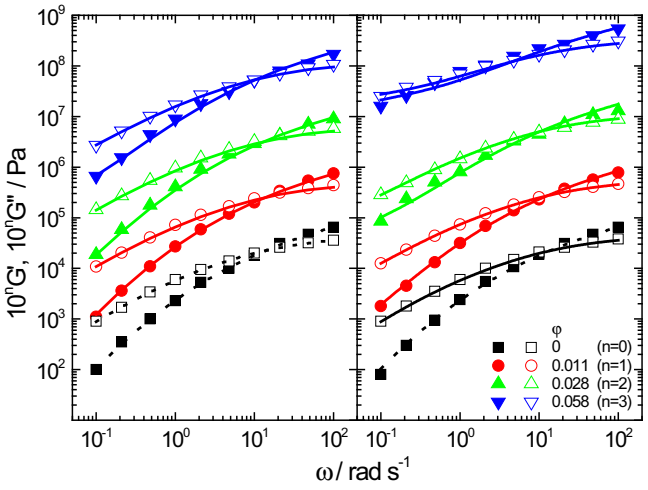

Fig. 3. G' (solid symbols) and G'' (hollow symbols) as a function of frequency ω at 200 °C for the CNF/PS nanocomposites prepared via the MB (a, left) and SC methods (b, right). The data of G' and G'' are vertically shifted by a factor of 10^n. G' and G'' were taken from Wang et al. [23]. The dotted curves are drawn according to least square fitting of Eq. (4) with $j = 3$ to the pure polymer and solid curves are calculated according to Eq. (5).

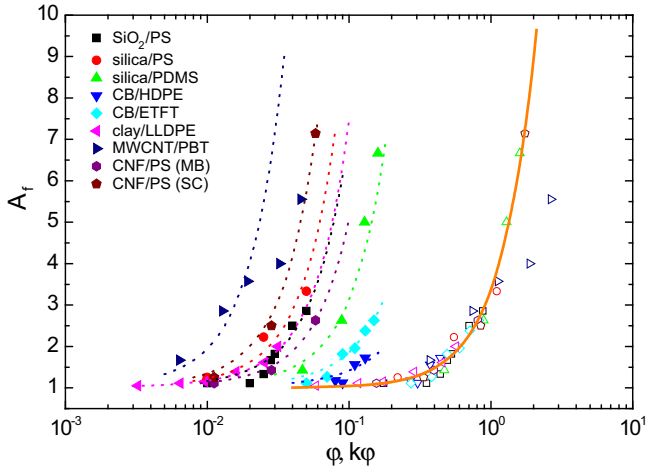

Fig. 4. A_f as a function of φ (filled symbols) and $k\varphi$ (hollow symbols) for different nanocomposites: CB/DHEP and CB/ETFT nanocomposites by our group [19], silica/PS nanocomposites by Havet and Isayev [20], silica/PDMS nanocomposites by Shim and Isayev [21], SiO_2/PS nanocomposites by Filippone et al. [22], clay/LLDPE nanocomposites by Durmus et al. [25], MWCNT/PBT nanocomposites by Wu et al., [24] and CNF/PS nanocomposites by Wang et al. [23]. The dotted curves are drawn according to Eq. (6) and the solid curve is drawn according to Eq. (8).

times that of pure polymer. Furthermore, Wang et al. assigned the dramatic changes in the SC nanocomposites at $\varphi = 0.058$ to the entanglements of CNF. Such viewpoints are rather popular in the literature. It is quite surprising that Eq. (3) could well account for the linear rheology of both the MB and the SC nanocomposites, indicating that the small change in fiber length from 4–60 μm to 1–20 μm does not causes any marked variation in the dynamics of the bulky phase of the matrix.

Interfacial tension between the filler and the matrix was calculated according to the geometric mean equation of Wu [71]. The interfacial tension is about 18.0 mN/m, 136.8 mN/m and 17.0 mN/m, respectively, for the pairs of CB–HDPE, SiO_2–PS and CNF–PS at the test temperatures. The fitting of Eq. (3) to the different nanocomposites in Figs. 1–3 reveals distinctly that the proposed model is applicable to a variety of experimental systems with different polymer-particle affinity and filler shapes. In fact, Eq. (3) is also applicable to the linear rheology of fumed silica/PS [20], precipitated silica/PDMS [21], clay/LLDPE [25], and MWCNT/PBT nanocomposites [24] in the terminal flow region. Restriction of large scale polymer relaxations by nanofillers has been used to account for the terminal plateaus [7,8,24]. However, the applicability of the proposed model to diverse nanocomposites allows addressing the following implications: (1) the effect of filler on the linear viscoelastic moduli is essentially the same for the systems considered; (2) the polymer shells immobilized onto the particle can be assumed as included in the filler phase for understanding the global viscoelasticity of filled polymers. It should be remarked that although the reinforcing mechanism of the filler is presumably different for each system due to the different polymer–filler affinity, Eq. (3) might mask the subtle rheological differences in the φ-dependent relaxation spectra [72]. Therefore, the four parameters, $A_f(\varphi)$, $G'_{f1}(\varphi)$, $G''_{f0}(\varphi)$ and α, should be examined to disclose the different reinforcing mechanism of the filler.

4. Discussion

Plotting $A_f(\varphi)$ against φ reveals a series of curves nearly parallel to each other for different composites except for the MWCNT/PBT nanocomposites at $\varphi > 0.03$, as shown in Fig. 4. $A_f(\varphi)$ has been interpreted as the Bueche expression [3], the Guth–Gold equation and its Padé approximation for spherical particle [31], the Guth–Gold function for asymmetric rod-like particle [26]

$$A_f(\varphi) = 1 + 0.67\,k\varphi + 1.62(k\varphi)^2 \tag{6}$$

or the Huber–Vilgis function for self-similar, rigid particle clusters [31,73,74] formed through a diffusion-controlled cluster–cluster aggregation (CCA) process [74].

$$A_f(\varphi) = 1 + C\varphi^{\frac{2}{3-d_f}} \tag{7}$$

Here, k is a shape factor defined as the length of the filler divided by its breadth, and C a constant related to size b of primary particles, and mean size ξ, anomalous diffusion exponent d_w and fractal dimension d_f of the filler cluster via $C \sim (\xi/b)^{d_w - d_f}$. Both Eqs. (6) and (7) could approximately account for the data in Fig. 4. The parameters k and d_f are estimated according to least square fitting of Eqs. (6) and (7), respectively, and the fitted values are listed in Table 1. Precipitated silica and CB as irregular aggregates by fusion of primary particles possess of typical k values ranged from 4 to 10 [75]. The other nanofillers exhibit rather large k values, indicating the formation of clusters with large aspect ratios. Specially, the k values of SiO_2 nanoparticles and fumed silica are as high as 17.6 and 22.0, respectively, indicating that Eq. (6) does not account for the shape factor of the filler particles but for the clusters. The k value of CNF in the SC nanocomposites is higher than that in the MB nanocomposites, being consistent with the variation of fiber length.

In nanocomposites, filler particles tend to aggregate in order to reduce the excess interfacial energy. The driving force for the agglomeration might arise from the strong dispersive interaction between the particle and the matrix as well as the depletion interaction between adjacent particles. The filler clustering results in non-trivial differences between filler volume fraction and cluster volume fraction due to the presence of the occluded polymer surrounding the filler inclusions. This concept is taken into account in Eq. (7) that contains a fractal dimension of the clusters. The d_f values in a narrow range from 1.67 to 2.00 are in agreement with the theoretical value 1.80 predicated for the self-similar CCA clusters. It is rather surprising that plotting of $A(\varphi)$ against $k\varphi$ reveals data collapse, except for the MWCNT/PBT nanocomposites at $\varphi > 0.03$. Though the d_f values are somewhat different for the

Table 1
Rheological parameters for different composites.

Composites	Characteristic of filler		Characteristic of matrix			T/°C[c]	k	d_f	x	y
	Nature and size	Special surface area/$m^2\ g^{-1}$	M_w/kg mol^{-1}	M_w/M_n	η_{m0}/kPa s					
SiO_2/PS[a] [22,71]	SiO_2/nanoparticle, diameter 14 nm	135–165	125	1.98	1.52	200	17.6 ± 0.8	1.99 ± 0.14	3.60 ± 0.26	3.00 ± 0.020
Fumed silica/PS[b] [20]	Diameter 20 nm	/	320	2.0	21.1	200	22.0 ± 1.2	2.00 ± 0.07	3.45 ± 0.06	3.11 ± 0.16
Precipitated silica/PDMS[a] [21]	Primary particle diameter 16 nm, agglomerate size 10 μm	200	414	1.77	5.46	80	10.4 ± 0.2	1.85 ± 0.18	4.77 ± 0.82	3.83 ± 0.57
CB/HDPE[a] [19]	Diameter 25 nm	63	/	/	19.2	160	3.4 ± 0.4	1.93 ± 0.04	3.11 ± 0.45	3.90 ± 0.42
CB/ETFT[a] [19]			/	/	26.8	260	5.5 ± 0.3	1.93 ± 0.14	2.77 ± 0.36	3.11 ± 0.45
Clay/LLDPE[a] [25]	Montmorillonite with 38% organic content	/	50		5.80	160	18.0 ± 0.5	1.67 ± 0.15	2.57 ± 0.19	2.72 ± 0.03
MWCNT/PBT[a] [24]	Outside diameter 10–20 nm, inside diameter 5–10 nm, length 10–30 μm	> 200	23.2	/	0.90	240	58.0 ± 2.9[d]	1.80 ± 0.10[d]	2.42 ± 0.28	2.74 ± 0.34
CNF/PS[a] [23]	Diameter 100–200 nm, length 1–20 μm	/	200	2.4	9.0	200	13.9 ± 0.3	1.90 ± 0.04	2.46 ± 0.36	2.24 ± 0.01
CNF/PS[b] [23]	Diameter 100–200 nm, length 4–60 μm	/				200	29.9 ± 0.4	1.98 ± 0.03	3.12 ± 0.30	3.63 ± 0.14

[a] Prepared using MB method.
[b] Prepared using SC method.
[c] Temperature where linear rheology is analyzed.
[d] Determined at $\varphi \leq 0.02$.

nanocomposites investigated, the collapsed data at $k\varphi < 1.7$ could be well described by a modified form of Eq. (7).

$$A_f(\varphi) = 1 + C(k\varphi)^{\frac{2}{3-d_f}} \tag{8}$$

with $d_f = 1.86 \pm 0.03$ ($R^2 = 0.98025$).

Fig. 5 shows $G'_{f1}(\varphi)$ and $G''_{f0}(\varphi)$ as a function of φ for the clay/LLDPE and the CB/ETFT nanocomposites as examples. The two characteristic moduli can be expressed as power laws

$$G'_{fl}(\varphi) \sim \varphi^x \tag{9}$$

and

$$G''_{f0}(\varphi) \sim \varphi^y \tag{10}$$

The scaling exponents x and y are determined according to least square fitting method, as listed in Table 1. The x and y values are in narrow ranges from 2.4 to 4.7 and from 2.2 to 3.9, respectively. The CCA models predict that equilibrium elastic modulus $G_0 = \lim_{\omega \to 0} G'(\omega)$ of filled polymers scales with φ [40,74,76]

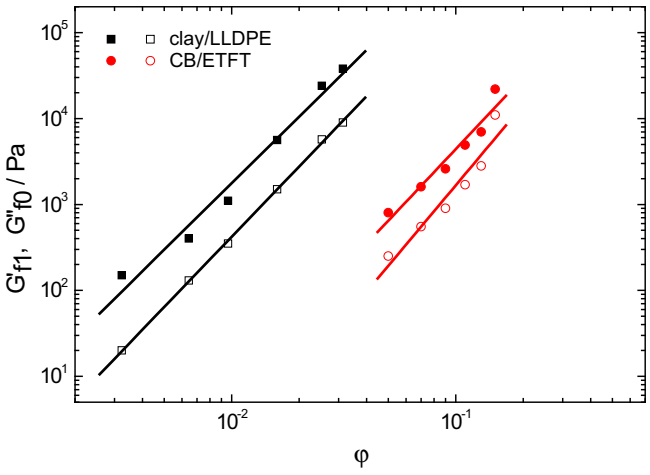

Fig. 5. G'_{f1} (solid symbols) and G''_{f0} (hollow symbols) as a function of φ for clay/LLDPE nanocomposites by Durmus et al. [25] and CB/ETFT nanocomposites by our group [19]. The straight lines are drawn according to Eqs. (9) and (10), respectively.

$$G_0 \sim \varphi^z \tag{11}$$

with an exponent $z \approx 3.5$ in case of particle fluctuation in their equilibrium positions [74,77]. Modulus measurement at small strains reveals that a certain category of filled polymers agrees with the predication of the CCA models [74,77–85]. However, a variety of systems exhibit rather high z values, for example, silica filled PDMS ($z = 7.2$) [86], liquid polyisoprene ($z = 5.2$) [87] and poly(ethylene oxide) ($z = 3.3$ at low silica contents and $z = 26.5$ at high silica contents) [88], as well as MWCNT filled polyisobutylene ($z = 7.1$) [89] and PDMS ($z = 6.7$) [90]. The z value is undoubtedly related to the frequency at which G' of filled polymers is evaluated. Values of $z = 1.0$ and $z = 3.4$ have been observed in the elastic plateau and the terminal regions in silica filled polybutadiene [85]. The present study allows picking up the characteristic moduli $G'_{f1}(\varphi)$ and $G''_{f0}(\varphi)$ associated with the filler phase. The x and y values might reflect the structural difference and the polymer–filler affinity of the nanocomposites.

Fig. 6 shows α as a function of $k\varphi$, disclosing a general tendency of α decay with increasing $k\varphi$. A glassy chain dynamics of $G' \sim \omega^{3/8}$ have been predicted for a certain strength of the filler activity [91]. However, the relaxation of the filler phase at high filler concentrations may be slower than the predicated glassy chains. This particular process is controlled by the frictional interaction between the absorbed chains and the particles, the density of the adsorbed chains on the surface of particles, and volume fraction of the interfacial layer in the "filler phase" [8]. It is worth noting that the variation of α against $k\varphi$ follows the same fashion for the CNF/PS nanocomposites prepared via the MB and the SC methods, indicating that the ω-dependence of the elastic component of the filler phase is related to both concentration and aspect ratio of the filler. The different α values from CB filled HDPE and ETFT suggest that this parameter is related to the polymer–filler affinity.

The time-concentration superposition (TCS) principle has been applied to weakly attracting colloid suspensions and filled polymers at controversy for about 30 years. Faitel'son and Yakobson [92] are the first to create TCS principle in dynamic rheology of liquid-like chalk dispersions at $\varphi \leq 0.15$ onto the dispersant (8% solution of polyisobutylene in cetane) using a modulus shift factor (call a_m here). a_m was also defined as "strain amplification factor" and it could be evaluated from the $|G^*|$ ratio of the suspension over the dispersant in the high-ω zone dominated by hydrodynamic

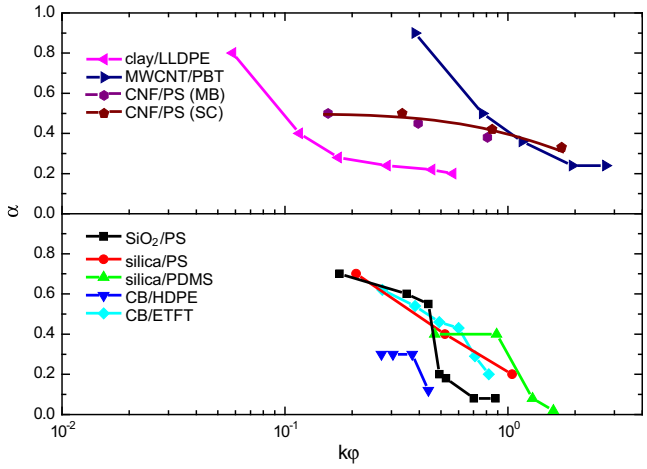

Fig. 6. α as a function of φ/φ_c for different composites.

forces [93]. Applicability of this TCS principle to several particle dispersions [93–95] suggests that the filler phase does not introduce any changes in dynamics of the dispersant, at least at φ below a percolation threshold φ_c in the high-ω zone. However, this TCS principle breaks down in the low-ω zone where the contribution from the particle network seems dominative. In fact, this TCS principle is only expected to the high-ω zone where the rheology is dominated by the polymer [96]. Trappe and Weitz [97] demonstrated another TCS principle in dynamic rheology of solid-like CB dispersions ($\varphi > \varphi_c$), by introducing two independent scaling factors for both modulus and frequency, a_m and a_ω, which is further validated in several dispersions and polymer composites [22,82,89,98–102]. The TCS attempts with two shift factors (a_m and a_ω) do establish master curves at $\varphi > \varphi_c$, disclosing the significance of filler network and its influence on polymer dynamics. Nevertheless, this TCS principle breaks down in the high-ω zone [22,99], being just opposite to the case at $\varphi < \varphi_c$ using only an a_m factor. The TCS breakdown is ascribed to the non-Newtonian feature of the polymer melts, whose relaxation modes are independent of filler content [72]. In the second TCS attempt, ω_{cr} and its corresponding modulus (G_{cr}) provide a convenient choice of a_ω and a_m [22,97,99], which undoubtedly fails for highly filled polymers with two $G'-G''$ crossovers or without $G'-G''$ crossover.

A more plausible TCS is obtained by Marcovich et al. [103] who scaled the dynamic rheology of wood flour filled polypropylene, by shifting along the frequency axis without any correction in modulus, to create master curve with neat polypropylene as the reference. In this case, the filler seems to impose on the chain dynamics in the whole composition. The TCS principles created so far are equivocal and could not connect with the present knowledge about chain dynamics and structural inhomogeneity in filled polymers [39,44]. Molecular dynamic simulation on an idealized nanofilled elastomer reveals the applicability of TCS principle to terminal relaxation on the chain length scale [104]. On the other hand, the TCS principle breaks down at the segmental length scale.

The proposed two phase model is consistent with the well-known structural inhomogeneity of filled polymers as well as the strain amplification and the filler clustering phenomena. The polymer can be divided into a rubbery bulk region far away from the filler and an absorbed shell close to the filler inclusions [55,56]. Dynamics of polymer chains in the rubbery bulk do not vary upon filler addition, which agrees with the conceptual treatment of the proposed two phase model. The bulk region behaves same as the unfilled polymer while its contribution to the viscoelasticity of the composites is enlarged due to the strain amplification or the hydrodynamic effect by the solid inclusions [1,26]. The expression of the proposed model (Eq. (3)) could be reduced to the TCS principle with an a_m factor provided that $G^*_f(\omega, \varphi)$ is negligible. The filler might impose on segmental relaxation of chains in the thin absorbed shell close to the fillers [41–43] to form bound and occluded polymers [52] and even a glassy lay [46–49], depending on the filler polymer–particle interactions [39,44]. The absorbed shell with chain immobilization, either physically or chemically originated, participates in the filler aggregates or CCA clusters, which constitutes the "filler phase" in the two phase model. The absorbed shell leads to an increase in effective filler volume fraction, which has already been taken into consideration in the CCA model [31,73,74].

The underlying physics of this model lies on the independent rheological responses of the polymer and the filler phases [105]. The two phase model is valid only if the filler clusters are stable within the frequency domain or at time scales shorter than the lifetime polymer–filler junctions [63]. It is undeniable that the two phase model with a given $A_f(\varphi)$ function fails in the nonlinear viscoelastic regime where a power-law cluster breakdown has been predicted [31,106].

5. Concluding remarks

Concerning the above discussion, the following concluding remarks seem pertinent: (1) the filler–polymer interaction and the possible interphase, if it exists, might be included in the filler phase for understanding the viscoelasticity of filled polymers; (2) the presence of the filler phase does not influence the polymer dynamics in the bulk phase far away from the filler. The applicability of the proposed model was also validated for the linear rheology of silica filled EPDM [107], CB filled EPDM [107,108] and polyisobutylene terpolymer [11], as well as nanoclay filled ethylene–propylene-diene terpolymer [107], nitrile rubber [109], and maleated ethylene–propylene rubber [110] in a wide φ range. Though the application of the proposed model was examined only to the nanocomposites in the present work, it is expected to work for polymers filled with both nano- and micron-sized fillers. The linear rheology of filled polymers is strongly influenced by topology and distribution of filler and the strength of filler–polymer interactions, which should be further investigated within the framework of the two phase model for gaining insight in the complex rheological behaviors of filled polymers. The physical meaning of the model shall become evident once the filler topology and the filler–polymer interactions are analyzed.

References

[1] Osman MA, Atallah A, Schweizer T, Ottinger HC. J Rheol 2004;48:1167–84.
[2] Ahmed A, Jones FR. J Mater Sci 1990;25:4933–42.
[3] Kraus G. Adv Polym Sci 1971;8:155–237.
[4] Shenoy AV. Rheology of filled polymer systems. Dordrecht, The Netherlands: Kluwer Academic Publishers; 1999.
[5] Wolthers W, vandenEnde D, Breedveld V, Duits MHG, Potanin AA, Wientjes RHW, et al. J Phys Rev E 1997;56:5726–33.
[6] Cassagnau P. Polymer 2008;49:2183–96.
[7] Osman MA, Atallah A. Polymer 2006;47:2357–68.
[8] Sarvestani AS, Jabbari E. Macromol Theor Simul 2007;16:378–85.
[9] Aranguren MI, Mora E, DeGroot JV, Macosko CW. J Rheol 1992;36:1165–82.
[10] Sternstein SS, Zhu AJ. Macromolecules 2002;35:7262–73.
[11] Yurekli K, Krishnamoorti R, Tse MF, Mcelrath KO, Tsou AH, Wang HC. J Polym Sci Part B Polym Phys 2001;39:256–75.
[12] Allegra G, Raos G, Vacatello M. Prog Polym Sci 2008;33:683–731.
[13] Li L, Masuda T. Polym Eng Sci 1990;30:841–7.
[14] Larson RG. The structure and rheology of complex fluids. New York: Oxford University Press; 1999.
[15] Mansoutre S, Colombet P, Van Damme H. Cement Concrete Res 1999;29:1441–53.
[16] Ancey C, Jorrot H. J Rheol 2001;45:297–319.
[17] Wang MJ. Rubber Chem Technol 1998;71:520–89.

[18] Bar-Chaput S, Carrot C. Rheol Acta 2006;45:339–47.
[19] Song Y, Zheng Q, Cao Q. J Rheol 2009;53:1379–88.
[20] Havet G, Isayev AI. Rheol Acta 2003;42:47–55.
[21] Shim SE, Isayev AI. Rheol Acta 2004;43:127–36.
[22] Filippone G, Romeo G, Russo P, Acierno D. In: AIP Conf. Proc, vol. 1042; 2008. p. 29–31.
[23] Wang YR, Xu JH, Bechtel SE, Koelling KW. Rheol Acta 2006;45:919–41.
[24] Wu DF, Wu L, Zhang M. J Polym Sci Part B Polym Phys 2007;45:2239–51.
[25] Durmus A, Kasgoz A, Macosko CW. Polymer 2007;48:4492–502.
[26] Mullins L, Tobin NR. J Appl Polym Sci 1965;9:2993–3009.
[27] Litvinov VM, Spiess HW. Die Makromol Chem 1992;193:1181–94.
[28] Westermann S, Kreitschmann M, PyckhoutHintzen W, Richter D, Straube E. Physica B: Condensed Matter 1997;234:306–7.
[29] Westermann S, Kreitschmann M, Pyckhout-Hintzen W, Richter D, Straube E, Farago B, et al. Macromolecules 1999;32:5793–802.
[30] Botti A, Pyckhout-Hintzen W, Richter D, Urban V, Straube E. J Chem Phys 2006;124:174908.
[31] Heinrich G, Kluppel M, Vilgis TA. Curr Opin Solid State Mater Sci 2002;6:195–203.
[32] Pryamitsyn V, Ganesan V. Macromolecules 2006;39:844–56.
[33] Reichert WF, Goritz D, Duschl EJ. Polymer 1993;34:1216–21.
[34] Wang Y, Wang JJ. Polym Eng Sci 1999;39:190–8.
[35] Friedlander SK, Jang HD, Ryu KH. Appl Phys Lett 1998;72:173–5.
[36] Friedlander SK, Ogawa K, Ullmann M. J Polym Sci Part B Polym Phys 2000;38:2658–65.
[37] Suh YJ, Friedlander SK. J Appl Phys 2003;93:3515–23.
[38] Suh YJ, Ullmann M, Friedlander SK, Park KY. J Phys Chem B 2001;105:11796–9.
[39] Bandyopadhyaya R, Rong WZ, Friedlander SK. Chem Mater 2004;16:3147–54.
[40] Potanin AA, Derooij R, Vandenende D, Mellema J. J Chem Phys 1995;102:5845–53.
[41] Simhambhatla M, Leonov AI. Rheol Acta 1995;34:329–38.
[42] Lee KJ, Lee DK, Kim YW, Choe WS, Kim JH. J Polym Sci Part B Polym Phys 2007;45:2232–8.
[43] Robertson CG, Roland CM. Rubber Chem Technol 2008;81:506–22.
[44] Schroder A, Kluppel M, Schuster RH. Macromol Mater Eng 2007;292:885–916.
[45] Gagliardi S, Arrighi V, Ferguson R, Telling MTF. Physica B: Condensed Matter 2001;301:110–4.
[46] Yim A, Chahal RS, St. Pierre LE. J Colloid Interf Sci 1973;43:583–90.
[47] Landry CJT, Coltrain BK, Landry MR, Fitzgerald JJ, Long VK. Macromolecules 1993;26:3702–12.
[48] Tsagaropoulos G, Eisenberg A. Macromolecules 1995;28:396–8.
[49] Tsagaropoulos G, Eisenberg A. Macromolecules 1995;28:6067–77.
[50] Litvinov VM, Spiess HW. Die Makromol Chem 1991;192:3005–19.
[51] Starr FW, Schroder TB, Glotzer SC. Macromolecules 2002;35:4481–92.
[52] Bogoslovov RB, Roland CM, Ellis AR, Randall AM, Robertson CG. Macromolecules 2008;41:1289–96.
[53] Sen S, Xie YP, Kumar SK, Yang HC, Bansal A, Ho DL, et al. Phys Rev Lett 2007;98:128302.
[54] Dutta NK, Choudhury NR, Haidar B, Vidal A, Donnet JB, Delmotte L, et al. Polymer 1994;35:4293–9.
[55] Berriot J, Montes H, Lequeux F, Long D, Sotta P. Macromolecules 2002;35:9756–62.
[56] Montes H, Lequeux F, Berriot J. Macromolecules 2003;36:8107–18.
[57] Sarvestani AS. Eur Polym J 2008;44:263–9.
[58] Leonov AI. J Rheol 1990;34:1039–68.
[59] Mujumdar A, Beris AN, Metzner AB. J Non-Newton Fluid 2002;102:157–78.
[60] Havet G, Isayev AI. Rheol Acta 2001;40:570–81.
[61] Kagarise C, Koelling KW, Wang YR, Bechtel SE. Rheol Acta 2008;47:1061–76.
[62] Sarvestani AS, Picu CR. Rheol Acta 2005;45:132–41.
[63] Sarvestani AS, Picu CR. Polymer 2004;45:7779–90.
[64] Merabia S, Sotta P, Long DR. Macromolecules 2008;41:8252–66.
[65] Robertson CG, Lin CJ, Rackaitis M, Roland CM. Macromolecules 2008;41:2727–31.
[66] Colombini D, Hassander H, Karlsson OJ, Maurer FHJ. Macromolecules 2004;37:6865–73.
[67] Moczo J, Pukanszky B. J Ind Eng Chem 2008;14:535–63.
[68] Privalko VP, Shumsky VF, Privalka EG, Karaman VM, Walter R, Friedrich K, et al. J Mater Process Technol 2003;137:208–13.
[69] Mele P, Marceau S, Brown D, de Puydt Y, Alberola ND. Polymer 2002;43:5577–86.
[70] Sarvestani AS. Int J Solids Struct 2003;40:7553–66.
[71] Wu S. Polymer interface and adhesion. New York: Marcel Dekker Inc; 1982.
[72] Romeo G, Filippone G, Russo P, Acierno D. Polym Bull 2009;63:883–95.
[73] Huber G, Vilgis TA. Kaut Gummi Kunstst 1999;52:102–7.
[74] Kluppel M. Adv Polym Sci 2003;164:1–86.
[75] Bergstrom JS, Boyce MC. Rubber Chem Technol 1999;72:633–56.
[76] Potanin AA, Russel WW. Phys Rev E 1996;53:3702–9.
[77] Cassagnau P. Polymer 2003;44:2455–62.
[78] Payne AR. J Appl Polym Sci 1963;7:873–85.
[79] Payne AR. J Appl Polym Sci 1964;8:2661–86.
[80] Meier JG, Kluppel M. Macromol Mater Eng 2008;293:12–38.
[81] Heinrich G, Kluppel M. Filled elastomers drug delivery systems, vol. 160; 2002. p. 1–44.
[82] Chatterjee T, Krishnamoorti R. Phys Rev E 2007;75:050403.
[83] Kluppel M, Heinrich G. Kaut Gummi Kunstst 2005;58:217–24.
[84] Piau JM, Dorget M, Palierne JF. J Rheol 1999;43:305–14.
[85] Zhu ZY, Thompson T, Wang SQ, von Meerwall ED, Halasa A. Macromolecules 2005;38:8816–24.
[86] Paquien JN, Galy J, Gerard JF, Pouchelon A. Colloid Surf A 2005;260:165–72.
[87] Gurovich D, Macosko CW, Tirrell M. Rubber Chem Technol 2004;77:1–12.
[88] Ponton A, Quemada D, Lafuma F, Neel O. Colloid Surf A 1996;119:255–9.
[89] Hobbie EK, Fry DJ. Phys Rev Lett 2006;97:0361011–4.
[90] Marceau S, Dubois P, Fulchiron R, Cassagnau P. Macromolecules 2009;42:1433–8.
[91] Vilgis TA. Polymer 2005;46:4223–9.
[92] Faitel'son LA, Yakobson ÉÉ. Mech Compos Mater St 1977;13:898–906.
[93] Gleissle W, Hochstein B. J Rheol 2003;47:897–910.
[94] Mongruel A, Cartault M. J Rheol 2006;50:115–35.
[95] Xu XM, Tao XL, Gao CH, Zheng Q. J Appl Polym Sci 2008;107:1590–7.
[96] Vermant J, Ceccia S, Dolgovskij MK, Maffettone PL, Macosko CW. J Rheol 2007;51:429–50.
[97] Trappe V, Weitz DA. Phys Rev Lett 2000;85:449–52.
[98] Daga VK, Wagner NJ. Rheol Acta 2006;45:813–24.
[99] Romeo G, Filippone G, Fernandez-Nieves A, Russo P, Acierno D. Rheol Acta 2008;47:989–97.
[100] Rahatekar SS, Koziol KK, Kline SR, Hobbie EK, Gilman JW, Windle AH. Adv Mater 2009;21:874–8.
[101] Hobbie EK, Fry DJ. J Chem Phys 2007;126:1249071–7.
[102] Jager KM, Eggen SS. Polymer 2004;45:7681–92.
[103] Marcovich NE, Reboredo MM, Kenny J, Aranguren MI. Rheol Acta 2004;43:293–303.
[104] Liu J, Cao DP, Zhang LQ, Wang WC. Macromolecules 2009;42:2831–42.
[105] Trappe V, Prasad V, Cipelletti L, Segre PN, Weitz DA. Nature 2001;411:772–5.
[106] Kluppel N. Macromol Symp 2003;194:39–45.
[107] Tan H, Isayev AI. J Appl Polym Sci 2008;109:767–74.
[108] Osanaiye GJ. J Appl Polym Sci 1996;59:567–75.
[109] Chung JW, Han SJ, Kwak SY. Compos Sci Technol 2008;68:1555–61.
[110] Austin JR, Kontopoulou M. Polym Eng Sci 2006;46:1491–501.